

# A MODIFIED SYNCHROTRON MODEL FOR KNOTS IN THE M87 JET

Wen-Po Liu<sup>1,2</sup>, Zhi-Qiang Shen<sup>1</sup>

## ABSTRACT

For explaining the broadband spectral shape of knots in the M87 jet from radio through optical to X-ray, we propose a modified synchrotron model that considers the integrated effect of particle injection from different acceleration sources in the thin acceleration region. This results in two break frequencies at two sides of which the spectral index of knots in the M87 jet changes. We discuss the possible implications of these results for the physical properties in the M87 jet. The observed flux of the knots in the M87 jet from radio to X-ray can be satisfactorily explained by the model, and the predicted spectra from ultraviolet to X-ray could be further tested by future observations. The model implies that the knots D, E, F, A, B, and C1 are unlikely to be the candidate for the TeV emission recently detected in M87.

*Subject headings:* galaxies: active — galaxies: individual (M87) — galaxies: jets — radiation mechanisms: non-thermal

## 1. Introduction

The giant radio galaxy M87, situated nearly at the center of the Virgo cluster at a distance of 16 Mpc (e.g. Macri et al. 1999), has been studied extensively from the radio (e.g., Owen et al. 1989 and references therein; Biretta et al. 1995; Sparks et al. 1996), optical (e.g. Perlman et al. 2001a, hereafter P01; Biretta et al. 1991), UV (Waters & Zepf 2005, hereafter WZ05), to X-ray (e.g., Marshall et al. 2002, hereafter M02; Wilson & Yang 2002). The predicted TeV gamma-ray (Bai & Lee 2001) and the possible position where the TeV emission from the M87 jet (Georganopoulos et al. 2005; Cheung et al. 2007) have also been confirmed at a high confidence level by the HESS observations (Aharonian et al. 2003 & 2006). In particular, Perlman & Wilson (2005, hereafter PW05) analyzed diagnostics

---

<sup>1</sup>Shanghai Astronomical Observatory, Shanghai 200030, P.R.China; wpliu@shao.ac.cn

<sup>2</sup>The Graduate School of Chinese Academy of Sciences, Beijing 100049, P.R.China

and physical interpretation of the X-ray emissions from the M87 jet in detail. Many other observations have also been done, such as photometric surveys of the jet, polarimetry maps of the jet (Perlman et al. 1999).

In the M87 jet, the Optical-X-ray spectral index  $\alpha_{\text{ox}}$  ( $S_\nu \propto \nu^{-\alpha}$ ) increases from  $1.2 - 1.4$  at  $2'' - 7''$  from the nucleus (knots D and E) to  $1.7 - 1.9$  at  $15'' - 18''$  from the nucleus (knots B and C1). The Chandra data confirm steep X-ray spectra of the knots in the M87 jet ( $\alpha_x > \alpha_r$ ) and are thus consistent with a synchrotron origin for the X-ray jet emission (M02; Wilson & Yang 2002; PW05). So far, there have been three standard theoretical synchrotron models. The KP model (Kardashev 1962, hereafter K62; Pacholczyk 1970) assumes that the source of the emission is a single burst of energetic electrons with an isotropic pitch-angle distribution and thus no scatters. Because of the likely scattering of relativistic particles by hydromagnetic waves (e.g., Wentzel 1977), the KP model is physically unreasonable, and therefore will not be mentioned further in this paper. The JP model (Jaffe & Perola 1973) assumes the same initial conditions as those of the KP model, but allows scattering in the pitch-angle distribution so that it can maintain an isotropic distribution all the time. The resulting spectrum is an essentially exponential rollover above the synchrotron loss break frequency. The continuous injection (CI) models (K62; Heavens & Meisenheimer 1987, hereafter HM87) assume that a power law distribution of relativistic particles is being continuously added to the emitting region, but the CI model of HM87 further takes the advective transport of the accelerated electrons downstream into account. The CI model of K62 has the similar spectral shape to the one of HM87.

But these synchrotron models also have some problems. As shown in WZ05, considering the X-ray flux, the CI model is only applicable for the inner knots (knots D and E), and explains the UV turnover (Fig 1), but for other outer knots (such as knots F and A) this model systematically over-predicts the observed UV turnover. And PW05 also found that such a model cannot explain the spectral index at X-ray. Without considering the X-ray data, the predicted X-ray flux by the CI model is higher than the observed one, but the exponential high-energy rollover of JP model underpredicts the X-ray flux by many orders of magnitude and the slope at X-ray is much larger than the observed. The two standard models can't fit the X-ray flux and the spectral index at X-ray under the single index of the electron energy spectrum at injection and single emission process. We summarize the criteria for fitting the spectral energy distributions (SEDs) of the knots in the M87 jet discussed in WZ05 and PW05: firstly, the first break frequency should be under the UV turnover (Fig 1), especially, for knots D, A, and B; secondly, a steeper X-ray spectral index than the optical is needed, so there may be a second break frequency between UV data and X-ray data; finally, the best fitting model should explain the flux and index of the X-ray data as well as the ones of the radio, optical and UV data.

In § 2, we describe in detail our modified synchrotron model for knots in the M87 jet. In § 3, we present and discuss the fitting results of this model to the wide-band spectra of the knots D, E, F, A, B, and C1. A summary is given in § 4.

## 2. The Model

We suggest a synchrotron model which is a modified CI model of K62, to explain the observed SEDs of the knots in the M87 jet. The kinetic equation of the relativistic electrons in the CI model (K62) is :

$$\frac{\partial N}{\partial t} = \beta \frac{\partial}{\partial E}(E^2 N) + qE^{-p}, \quad (1)$$

where  $\beta = bB_{\perp}^2$ ,  $b$  is a constant,  $B_{\perp}$  represents the component of the magnetic field perpendicular to the velocity of the particle. The synchrotron energy losses are  $dE/dt = -\beta E^2$ . The injection of a constant spectrum  $qE^{-p}$  in the CI model of K62 actually implies that the acceleration region is the same as the main emission region in the knots. However, this assumption may not be true in general, especially for shocks acceleration mechanism which may be the dominant mechanism of the particle acceleration in jets. Based on the observational evidence of shocks in the M87 jet (Perlman et al. 1999; PW05; Harris & Krawczynski 2006), a more physical scenario would be that the acceleration region and the main emission region are not strictly co-spatial in the M87 jet, and the accelerated injection electrons may be advected downstream (this process is similar to the CI model of HM87). The electrons advection throughout the jet and diffusion throughout the jet's cross-section with the decrease of the synchrotron lifetimes from low energies to high energies may result in spatially stratified emission regions along the jet (M02) and the consistent narrowing of the jet from radio to optical to X-ray (PW05). For the acceleration region, a more complex but physical scenario may be that there are many acceleration sources in a compact acceleration region which is unresolved by the telescope beam and each source has a power law distribution of injection population of relativistic electrons. We assume that all the sources accelerate electrons under the similar conditions (e.g., similar magnetic fields etc.) with the same mechanism which results in a same spectral index  $p$ , similar electron number density, the same maximum energy and fluid velocity for the injection populations of relativistic electrons into the main emission region. Before injecting into the main emission region, the populations of relativistic electrons in the acceleration region will experience a brief synchrotron loss process. But the observed knot emission is dominated by the emission from the main emission region. If the injection electrons into the main emission region come from a very compact

region, not resolved by the observation, we need to integrate all the contributions of populations from different locations of the acceleration region by considering synchrotron losses. We assume that  $r$  is the distance to the main emission region from a source of the acceleration region. At low energies, the populations from different locations of the acceleration region have the same spectral shape, so the integrated injection spectrum of the electrons over the acceleration region still scales as  $E^{-p}$ . At higher energies, the electrons are advected a distance  $r$  to the main emission region before losing a significant fraction of their energy to synchrotron emission. As the loss time-scale scales as  $E^{-1}$ , this distance scales as  $E^{-1}$ . Thus the integrated injection spectrum at high energies would be proportional to  $E^{-(p+1)}$ . There is a break energy  $E_b$  between the low energies and the high energies in the integrated injection spectrum. The integrated injection spectrum exhibits a cut-off energy  $E_c$ . By adding up the contributions from sources in the acceleration region, the integrated injection spectrum as the source into the main emission region from the acceleration region can be written as,

$$\begin{cases} q_1 E^{-p}, & E < E_b ; \\ q_2 E^{-(p+1)}, & E_c > E > E_b ; \\ 0, & E > E_c , \end{cases} \quad (2)$$

where,  $q_2 E^{-(p+1)}$  corresponds to the component of the injection spectrum at high energies. The spectrum near the break energy in fact is not a strict power law, and the equivalent spectral index should be intermediate. But here we would simply consider a power law form for the spectrum. The real distribution of the electrons and the magnetic field in the M87 jet is very complex (M02; Perlman et al. 1999; Perlman et al. 2001b), but we simply assume that the distribution of the electrons is isotropic and the large-scale equipartition magnetic field in the main emission region is approximately symmetrical. The kinetic equation is:

$$\frac{\partial N}{\partial t} = \beta \frac{\partial}{\partial E} (E^2 N) + \begin{cases} q_1 E^{-p}, & E < E_b ; \\ q_2 E^{-(p+1)}, & E > E_b . \end{cases} \quad (3)$$

Then, we have

$$N(E, \theta, t) = \begin{cases} \frac{q_1 E^{-(p+1)}}{\beta(p-1)} [1 - (1 - \beta E t)^{p-1}], & E < \frac{1}{\beta t} ; \\ \frac{q_1 E^{-(p+1)}}{\beta(p-1)}, & E_b > E > \frac{1}{\beta t} ; \\ \frac{q_2 E^{-(p+2)}}{\beta p}, & E > E_b . \end{cases} \quad (4)$$

For isotropic distributions, we can derive the flux expression of the modified synchrotron model

$$I_\nu \propto \begin{cases} \nu^{-(p-1)/2}, & \nu \ll \nu_{B1} ; \\ \nu^{-p/2}, & \nu_{B2} > \nu \gg \nu_{B1} ; \\ \nu^{-(p+1)/2}, & \nu > \nu_{B2} . \end{cases} \quad (5)$$

$$\nu_{B1} = c_3 t^{-2}, \nu_{B2} = c_3 \beta^2 E_b^2, c_3 = 3.4 \times 10^8 B^{-3},$$

where  $t$  (in yr) is synchrotron lifetime,  $\nu_{B1}$  and  $\nu_{B2}$  (in Hz) are the first and second break frequencies, respectively.

### 3. Fitting Results and Discussion

Now, we apply the above modified synchrotron model to the observed knot emission in the M87 jet. These include knots D, E, F, A, B, and C1 (as showed in Figure 1 of Harris & Krawczynski 2006).

The data we used are listed in Table 1. These include the published radio to UV data (P01), UV data at  $1.8 \times 10^{15}$  Hz (WZ05) and X-ray data (PW05). There is another reported X-ray measurement (M02) made 12 days before PW05 observation. M02 did not use the same regions to integrate the fluxes for various components as did P01. PW05, however, did use the same regions as P01, so we use PW05 data points in our model fitting. There was no X-ray measurement for the knot C1. So we estimated its flux density using the measurements for the knot C and the ratio of knots C1 to C from the optical observation at  $1.0 \times 10^{15}$  Hz by assuming this ratio is the same at both optical ( $1.0 \times 10^{15}$  Hz) and X-ray. There were no error bars in the X-ray data by PW05. The error bars for the PW05 X-ray data listed in Table 1 were estimated by assuming the same relative precision (the uncertainty in terms of a fraction of the value of the result) in both PW05 and M02 data. We use the weighted least square method to fit our model (Equation 5) to the wide-band data in each knot, in this progress a power law form is chosen near the break frequencies because we only need to concern the trend of the break frequencies. There are two peak frequencies in our model, but we don't know where they are when we fit our model to the broadband data in each knot. So we first arbitrarily divide broadband data into three groups to perform the least square method, we could calculate the corresponding reduce chi square ( $\chi_\nu^2$ ) by changing the division. All the possible combinations are considered before we obtain the best fit with a minimal  $\chi_\nu^2$  among them. These best-fit parameters for each knot, are listed in Table 2. The SEDs for the knots in the M87 jet and the best fits for our model are plotted in Fig 1.

Our model can well fit the radio, optical, UV, and X-ray data for these knots with three

segments except knot E which has two segments implying that the second break frequency of knot E has exceeded the X-ray band. It satisfies the aforementioned three constraints for the SED of the knots of M87 jet (as shown in Fig 1 and Table 2). The predicted spectra shape of knots from UV to X-ray (from  $-p/2$  to  $-(p+1)/2$ ) could be tested by future telescope in the band. The equivalent spectral index of the high energy electrons in the acceleration region may not decay from  $p$  to  $p+1$ , but is likely to be between them (i.e. the high energy electrons may be near the break energy). This results in an equivalent spectral index of the photons possibly between  $p/2$  and  $(p+1)/2$  (e.g. knot D). Our model is consistent with the spectral indexes of the knots E, F, A, B, and C1 within their error bars.

The first break synchrotron frequencies ( $\nu_{B1}$ ) of all the knots (D, E, F, A, B, and C1) in the M87 jet are under  $10^{15}$  Hz (see Table 2). According to the unified scheme of AGNs and equation (1) in Bai & Lee (2001), the Compton components from these knots will peak at  $0.01 \sim 1$  GeV, and their flux densities at TeV would be undetectable (based on the synchrotron self-Compton model and the equation (4) in Bai & Lee 2001). This implies that the knots D, E, F, A, B, and C1 are unlikely to be the candidate for TeV emission in the M87 detected by the HESS observations (Aharonian et al. 2003 & 2006). The possible candidate for the TeV emission in M87 is related to the innermost region of M87 like HST-1 or core itself (Stawarz et al. 2006; Aharonian et al. 2006; Cheung et al. 2007). HST-1, the knot closest to the core of M87, has been shown to have a very dynamic light curve and flaring (Perlman et al. 2003; Harris et al. 2003; Stawarz et al. 2006; Harris et al. 2006). Its mechanism may be related to the core and thus more complicated.

From Table 2, as a whole the second break frequency  $\nu_{B2}$  decreases along the jet. This may imply that the synchrotron loss in the acceleration region will increase along the jet.

We find that the value of the particle spectral index  $p$  is about 2.36 on average, which agrees well with the latest expectations from both diffusive shock acceleration theory (2.0-2.5, Kirk & Dendy 2001) and acceleration by relativistic shocks (2.23 in the ultrarelativistic limit, Kirk 2002). Particle acceleration at shocks (e.g., Blandford & Ostriker 1978) through the first-order Fermi process is generally believed to occur in jets.

PW05 proposed a possible phenomenological model to modify the CI model. They suggest that the filling factor of the volume within which particles are accelerated declines with increasing energy at X-ray energy along the jet (not in the direction perpendicular to the jet), but they can't explain the running mechanism of filling factor. To explain the curved X-ray spectra of BL Lac objects, Perlman et al. (2005) consider an episodic particle acceleration model which assumes only a time-variable particle acceleration. This results in a logarithmic curvature rather than a sudden break and could be related to the broadband spectral shape too. Fleishman (2006) suggests a very different model which explicitly takes

into account the effect of the small-scale random magnetic field, probably present in the M87 jet. But the energy densities contained in small-scale and large-scale magnetic fields may be incomparable, we think that the electrons in the large-scale magnetic field could also give rise to emission of the knots in our model, especially at high frequencies. The idea of a secondary population of the relativistic electrons that have different spectral index from the first population is discussed by Jester et al. (2005), which is partially similar to our model. But we consider a lot of populations of relativistic electrons that have the same spectral index in the acceleration region and discuss the detailed process that may be responsible for the knots in the M87 jet.

#### 4. Conclusion

We propose a modified CI model that considers a decay of spectral index of injection electrons possibly due to the sum of the injection spectrum from different acceleration sources with synchrotron losses in the thin acceleration region, so there are two break frequencies at two sides of which the spectral index changes for the spectra of knots in the M87 jet. We consider that the emission of the knot may be still emitted by the relativistic electrons in the large-scale magnetic field at high frequencies as well as the low frequencies, but not by the small-scale random magnetic field (e.g., Fleishmann 2005). Our model gives a satisfactory fit to the SEDs of knots in the M87 jet. Based on our analysis, the knots D, E, F, A, B, and C1 are unlikely to be responsible for the TeV emission detected in M87. The fitting results from our model imply that the particles in M87 are accelerated by shocks, and as a whole the second break frequencies of knots decrease down the jet. We also predict the spectra of knots from UV to X-ray, which could be tested by future observations in the band.

We thank C. Z. Waters for helpful communications and supplying his code to us for reference. Many thanks are due to the referee for the critical and constructive comments, which improved our work greatly. This work was supported in part by the National Natural Science Foundation of China (grants 10573029, 10625314, and 10633010) and the Knowledge Innovation Program of the Chinese Academy of Sciences (Grant No. KJCX2-YW-T03), and sponsored by the Program of Shanghai Subject Chief Scientist (06XD14024). Z.-Q. Shen acknowledges the support by the One-Hundred-Talent Program of the Chinese Academy of Sciences.

## REFERENCES

- Aharonian, F. et al. 2003, A&A, 403, L1
- Aharonian, F. et al. 2006, Science, 314, 1424
- Bai, J. M., & Lee M. G. 2001, ApJ, 549, L173
- Biretta, J. A., Stern, C. P., & Harris, D. E. 1991, AJ, 101, 1632
- Biretta, J. A., Zhou, F., & Owen, F. N. 1995, ApJ, 447, 582
- Blandford, R. D., & Ostriker, J. P. 1978, ApJ, 221, L29
- Cheung, C. C., Harris, D. E., & Stawarz, L. 2007, ApJ, 663, L65
- Fleishman, G. D. 2006, MNRAS, 365, L11
- Georganopoulos, M., Perlman, E. S., & Kazanas, D. 2005, ApJ, 634, L33
- Harris, D. E, Biretta, J. A., Junor, W., Perlman, E. S., Sparks, W. B., & Wilson, A. S. 2003, ApJ, 586, L41
- Harris, D. E., et al. 2006, ApJ, 640, 211
- Harris, D. E., & Krawczynski, H. 2006, ARA&A, 44, 463
- Heavens, A. F., & Meisenheimer, K. 1987, MNRAS, 225, 335 (HM87)
- Jaffe, W. J., & Perola, G. C. 1973, A&A, 26, 423
- Jester, S., Röser H.-J., Meisenheimer, K., Perley R. 2005, A&A, 431, 477
- Kardashev, N. S. 1962, SvA (AJ), 6, 317 (K62)
- Kirk, J. G., & Dendy, R. O. 2001, J. Phys. G, 27, 1589
- Kirk, J. G. 2002, in “Particles and Fields in Radio Galaxies”, ASP Conference Series 250 (ASP: San Francisco), ed. R. A. Laing & K. M. Blundell, p. 41
- Macri, L. M., et al. 1999, ApJ, 521, 155
- Marshall, H. L., et al. 2002, ApJ, 564, 683 (M02)
- Owen, F. N., Hardee, P. E., & Cornwell, T. J. 1989, 340, 698
- Pacholczyk, A. G. 1970, Radio Astrophysics (San Francisco: Freeman)



- Perlman, E. S., Biretta, J. A., Zhou, F., Sparks, W. B., & Macchetto, F. D. 1999, *AJ*, 117, 2185
- Perlman, E. S., Biretta, J. A., Sparks, W. B., Macchetto, F. D., & Leahy, J. P. 2001a, *ApJ*, 551, 206 (P01)
- Perlman, E. S., et al. 2001b, *ApJ*, 561, L51
- Perlman, E. S., Harris, D. E., Biretta, J. A., Sparks, W. B., & Macchetto, F. D. 2003, *ApJ*, 599, L65
- Perlman, E. S. et al. 2005, *ApJ* 625, 727
- Perlman, E. S., & Wilson, A. S. 2005, *ApJ*, 627, 140 (PW05)
- Sparks, W. B., Biretta, J. A., & Macchetto, F. 1996, *ApJ*, 473, 254
- Stawarz, Ł., Aharonian, F., Kataoka, J., Ostrowski, M., Siemiginowska, A., & Sikora, M. 2006, *MNRAS*, 370, 981
- Riess, A. 2000, WFPC2 Instrument Sci. Rep. 00-04 (Baltimore: STSci)
- Wilson, A. S., & Yang, Y. 2002, *ApJ*, 568, 133
- Waters, C. Z., & Zepf, S. E. 2005, *ApJ*, 624, 656 (WZ05)
- Wentzel, D. G. 1977, *JGR*, 82, 714

Table 1. Flux Densities of Knots in the M87 Jet

Frequency $\nu$ (Hz)	Flux Density						Observing Date	Reference
	D	E	F	A	B	C1		
<i>VLA</i> (mJy):								
$1.50 \times 10^{10}$	$161.54 \pm 1.92$	$48.05 \pm 0.81$	$144.90 \pm 1.86$	$1218.00 \pm 12.00$	$808.40 \pm 8.30$	$544.70 \pm 5.60$	94 Feb 04	P01
<i>HST</i> ( $\mu$ Jy):								
$1.45 \times 10^{14}$	$280 \pm 11$	$71.4 \pm 3.0$	$262 \pm 11$	$2633 \pm 105$	$1739 \pm 70$	$971 \pm 39$	98 Apr 04	P01
$1.87 \times 10^{14}$	$224 \pm 9$	$67.2 \pm 2.0$	$271 \pm 11$	$2344 \pm 90$	$1489 \pm 60$	$797 \pm 32$	98 Feb 26	P01
$2.66 \times 10^{14}$	$168 \pm 7$	$42.9 \pm 2.3$	$147 \pm 6$	$1829 \pm 73$	$1104 \pm 44$	$606 \pm 24$	98 Feb 26	P01
$3.75 \times 10^{14}$	$150 \pm 4$	$42.3 \pm 1.3$	$158 \pm 5$	$1363 \pm 34$	$811 \pm 20$	$415 \pm 10$	98 Feb 25	P01
$4.50 \times 10^{14}$	$117 \pm 3$	$33.4 \pm 0.9$	$123 \pm 3$	$1086 \pm 27$	$623 \pm 16$	$310.7 \pm 7.8$	98 Feb 25	P01
$6.58 \times 10^{14}$	$96.2 \pm 2.5$	$28.0 \pm 0.8$	$98.8 \pm 2.6$	$904 \pm 23$	$504 \pm 13$	$241.0 \pm 6.1$	98 Feb 25	P01
$1.00 \times 10^{15}$	$59.5 \pm 1.6$	$16.2 \pm 0.6$	$62.7 \pm 1.7$	$586 \pm 15$	$306.8 \pm 7.8$	$135.9 \pm 3.5$	98 Feb 25	P01
$1.80 \times 10^{15}$	$26.7 \pm 0.9$	$10.0 \pm 0.9$	$34.5 \pm 1.7$	$275.2 \pm 12.7$	$147.4 \pm 7.9$	$80.8 \pm 12.9$	01 Feb 23	WZ05
<i>Chandra</i> (nJy):								
$2.42 \times 10^{17}$	$51.5 \pm 4.2$	$32.2 \pm 6.5$	$20.1 \pm 5.2$	$156 \pm 8.8$	$30.3 \pm 5.5$	$14.6^a \pm 5.2$	00 Jul 29	PW05 <sup>b</sup>

<sup>a</sup>The X-ray flux density of knot C1 was estimated by assuming the same flux ratio of the knot C1 to the knot C at both optical ( $1.00 \times 10^{15}$ ) Hz and X-ray band.

<sup>b</sup>The error bars for the PW05 X-ray data were estimated by assuming the same relative precision in both PW05 and M02 data (see text).

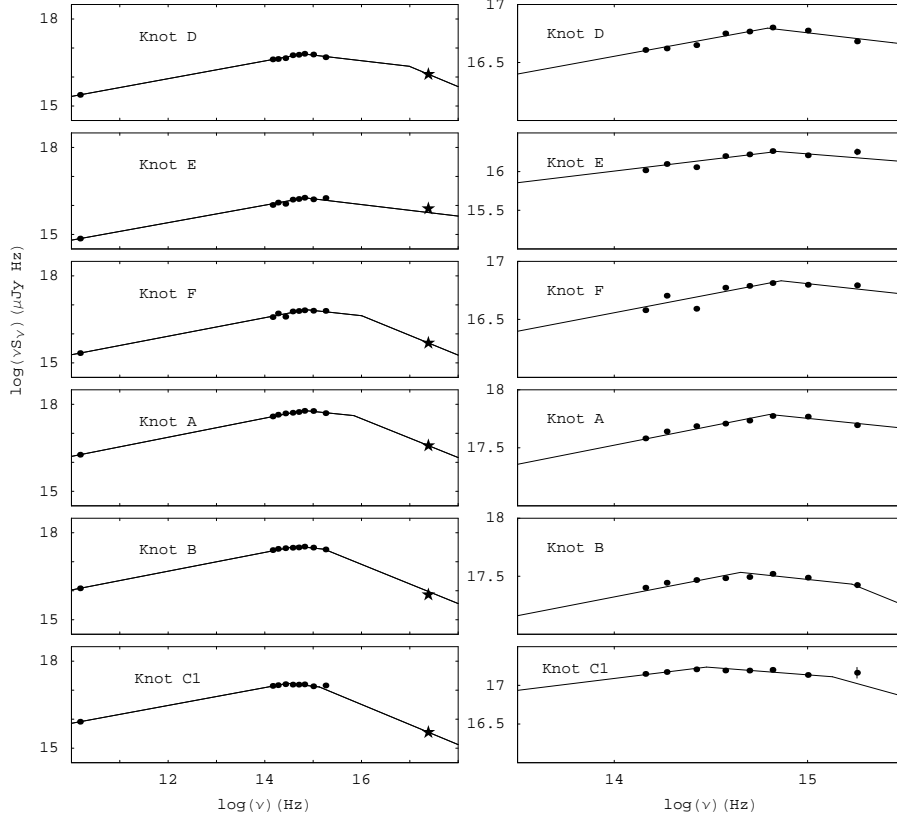


Fig. 1.— Left panel: plot of the SEDs for the knots in the M87 jet from radio through X-ray wavelengths. Right panel: plot zooming in on the optical and UV region, where most of the data points are and also where most of the curvature is. The data from radio to UV are plotted as filled circles, the X-ray data from PW05 as filled star. The solid lines display model fits that include the X-ray data from PW05. The error bars of most measurements are too small to be seen here. The best-fit parameters are listed in Table 2.

Table 2. Parameters for Model Fits for Radio through X-ray Data

Parameter	$\nu_{B1}(10^{14}\text{Hz})$	$\nu_{B2}(10^{15}\text{Hz})$	$p$	$\chi^2_\nu$
knot D	6.21	97.5	2.39	2.34
knot E	6.97	...	2.40	3.73
knot F	7.30	10.1	2.36	9.33
knot A	6.35	6.94	2.34	1.89
knot B	4.50	1.69	2.35	4.39
knot C1	3.00	1.34	2.38	2.55

Note. — Col. (1): Knot designation. Col. (2): First break frequency in  $10^{14}$  Hz. Col. (3): Second break frequency in  $10^{15}$  Hz. Col. (4): Spectral index of electrons. Col. (5): Reduced chi square.